Environmental Science Advances

ROYAL SOCIETY OF CHEMISTRY

PAPER

View Article Online
View Journal

Cite this: DOI: 10.1039/d5va00281h

Augmenting manure solids as scaffolding for phosphorus release/retention *via in situ* iron-phosphate complexes procured with Fe-biochar + $FeCl_3$ treatment

Krishna Yadav, † Chumki Banik and Santanu Bakshi *

Swine manure mismanagement can lead to several environmental issues, such as eutrophication and gaseous emissions. This study examines swine manure solid separation using a coagulant (0.15 M $FeCl_3$) with unmodified and iron-modified corn stover biochar, and evaluates phosphorus (P) recovery efficiency from the separated solids using Mehlich-III, Olsen, and citrate-bicarbonate-dithionite (CBD) extractants. Adding a combination of 0.15 M $FeCl_3$ and iron-modified biochar to manure effectively separated 100% P from the solution into the solid fraction by forming a strong iron phosphate (P^-) complex using inner-sphere and cation-bridging mechanisms. The spontaneity and feasibility of the process were assessed through a change in the Gibbs' free energy (ΔG^0), which was determined to be -23.3 kJ mol^{-1}. We evaluated the nutrient stability of the manure solid fraction using conductometric and pH metric analyses, and Mehlich-III solution in the presence of a dispersive medium (0.15 M NaCl), and the manure was characterized using Raman and FTIR spectra. Furthermore, the release pattern of macronutrients was determined by the degree of dissociation under the influence of different extractants. It is worth mentioning that CBD successfully extracted P (7477 mg kg^{-1}) from cation-bridged P^- and iron-bound P^-. This study presents an effective technique to separate P into solid fractions and offers a promising strategy for P recovery.

Received 20th August 2025
Accepted 27th October 2025

DOI: 10.1039/d5va00281h

rsc.li/esadvances

Environmental significance

This study highlights a sustainable approach to nutrient recovery from Fe-stabilized swine manure solids by demonstrating the superior efficacy of citrate-bicarbonate-dithionite (CBD) in mobilizing recalcitrant phosphorus (P) bound through complex iron interactions. Unlike conventional extractants, CBD leverages redox-driven mechanisms such as Fe^{3+} reduction and Fe^{2+} chelation to disrupt mineral-bound P phases, thereby significantly enhancing P availability. This work advances our understanding of environmental sciences related to phosphorus chemistry in waste matrices and promotes more effective strategies for nutrient recycling, aligning with circular bioeconomy and sustainable waste management goals.

1 Introduction

Swine manure is frequently introduced into soil in place of chemical fertilizers to boost crop productivity and reduce agricultural expenses. Utilizing swine manure has several additional advantages, including its low-cost availability and ability to add organic matter and enhance the soil's physical and biological characteristics.[1] However, the overapplication of swine manure to soil can lead to nutrient imbalance, water contamination, emission of greenhouse gases, and accumulation of heavy metals.[2,3] Therefore, it is imperative to employ effective pretreatment strategies to reduce the issues related to the overapplication of swine manure to the agricultural fields.

Among the several available pretreatment methods, the solid–liquid separation technique has been widely acknowledged in the literature.[4] This method can produce a solid fraction rich in phosphorus (P) fertilizer and a liquid fraction rich in nitrogen (N as NH_4^+) and potassium (K) at the expense of coagulants. In our previous study, we tested various coagulants ($FeCl_3$, HCl, and H_3PO_4) with iron-modified corn stover biochar for the solid–liquid separation of swine manure.[5] Among the coagulants tested, $FeCl_3$ was more efficient than the others, successfully separating 93% P from swine manure, of which 12% P was recycled using the Mehlich-III extractant. The optimum separation of P (93%) in the solid fraction and less recycling of P (12%) motivated us to evaluate the processes involved in P association and its release with biochar and manure colloids.

Bioeconomy Institute, Iowa State University, Ames, IA 50011, USA. E-mail: santanubakshi@gmail.com; Tel: +1 515-294-4984

† Present address: Department of Chemistry, School of Applied Sciences and Humanities, Vignan's Foundation for Science, Technology and Research, Vadlamudi, Guntur 522213, Andhra Pradesh, India.

A literature survey revealed several studies that employed biochar to remove P from simulated wastewater and swine farm wastewater.[3,5–9] Biochar derived from coniferous forest biomass showed low P sorption capacity (300 mg kg^{-1}) while modification with 2% iron increased the sorption capacity (2000 mg kg^{-1}).[10] The P sorbed on the unmodified biochar from coniferous forests showed high release (~35% of total P released), while iron-modified biochar released only ~4% of the total P.[10]

Several factors influence the retention of P by biochar and manure colloids (MC), such as solution pH, the mineralogical composition of manure solids, and association with macronutrients (Fe, Ca, and Mg). It has been found that MC, consisting of humic acid, lipids, and peptides, stabilized P when bound to mineral surfaces.[11–13] MC forms a strong organo-mineral complex through anion exchange with –OH groups on mineral surfaces, carboxyl groups, or phenolic groups of the MC.[14] The complexation of MC on mineral surfaces occurs primarily through ligand exchange mechanisms, which are favored under acidic conditions (with peak at a pH 4.3–4.7). This pH range corresponds to the pK_a values of most carboxylic acids and organic carboxyl groups, where surface complexation is most efficient.[15] Solution pH also affects their degree of dissociation by changing the positive or negative charges of the charged groups in the complex. Colloidal interactions and metal ions may lead to polyvalent cation bridging. The MC cations (Fe, Ca, and Mg) interact with MC anions $–COO^-$ and maintain neutrality on the surface by neutralizing the charge on both the negatively charged MC and phosphate ion (P^-), acting as a bridge.[15] Moreover, ionic strength (IS) and zeta potential (ZP) strongly influence P^- complex stability and ligand exchange efficiency. The IS plays an important role in the degree of electrostatic binding and structure of the cation-bridged manure colloid-P^- complex.[16–18] Kumar *et al.*[19] employed iron-modified biochar in P^- transport and reported that high IS influenced P^- sorption. Zeta potential is a measure of the surface potential and includes the particle surface and the potential at the shear plane.[20] Zeta potential provides important insights into the suspension stability of the manure solids in various solution conditions. Iron-modified biochar has been used for P^- removal from water, where a decrease in solution pH resulted in a decrease in ZP due to the adsorption of OH^- by biochar during pH adjustment with NaOH.[21,22] Based on the results of these studies, we inferred that experiments using solutions with different pH values, ZPs, and ISs can provide important insights into the mechanism of P association with MC.

Herein, we have adopted ferric chloride ($FeCl_3$) as a coagulant for the solid–liquid separation of swine manure and present four conditions as follows: (i) freeze-dried swine manure, (ii) swine manure with 0.15 M $FeCl_3$ solution (without biochar addition), (iii) swine manure mixed with corn stover-derived biochar followed by the addition of 0.15 M $FeCl_3$ solution, and (iv) swine manure mixed with iron-modified corn stover biochar followed by the addition of 0.15 M $FeCl_3$ solution. We selected the combination of coagulant and biochar based on its ability to adjust manure pH, strong coagulating properties, improvement of nutrient solubility, and the potential to concentrate the P in the solid fraction. The specific objectives of this study were to (i) assess the effects of biochar, $FeCl_3$, and a combination of biochar and $FeCl_3$ on P release due to cation and ligand bridging; and (ii) evaluate the P availability by changing H^+/OH^- activity. We hypothesized that the addition of biochar and $FeCl_3$ to swine manure would enhance P separation through cation bridging and the formation of inner-sphere complexes that immobilize P in the manure solid fraction, thereby decreasing its extractability with traditional extractants. We further hypothesized that altering the experimental pH conditions might influence the availability of P by disrupting its binding and increasing its solubility through different reaction mechanisms.

2 Materials and methods

2.1. Materials used in this study

The corn stover biomass was converted into biochar for this study using an autothermal fast pyrolyzer run at 500 °C with an ample air supply, keeping the equivalence ratio constant (12%). The biochar (BC) modification involved ferrous sulfate, and detailed information related to the preparation and modification of biochar was provided in our previously published paper.[23] The unmodified biochar is called control biochar (CB), and the biochar modified with ferrous sulfate is called iron biochar (IB).

The swine manure was collected from a commercial swine finishing barn in North Central Iowa. The manure collection details are provided elsewhere.[24] For manure solids, the swine manure was freeze-dried using a freeze dryer (Labconco benchtop) for 36 h with 0.04 mbar pressure, and the temperature was kept at −40 °C. The solid–liquid separation of swine manure was done using 0.15 M $FeCl_3$. We selected $FeCl_3$ based on our previous study and the high solubility of $FeCl_3$ compared to the ferric sulfate salt.[3] Initially, 0.15 M $FeCl_3$ solution was prepared separately using 80.1 g of $FeCl_3 \cdot 6H_2O$ salt in 2 L of distilled water using a 2 L volumetric flask. For the solid–liquid separation process, we utilized three different treatments. All treatments received 2 L of swine manure and 3 L of 0.15 M $FeCl_3$ solution; the only difference was 0 g BC, 20 g CB, and 20 g IB for the first, second, and third treatments, respectively. The resulting mixture was stirred adequately for 1 h using a magnetic stirrer and then kept at room temperature (23 °C) for 24 h to achieve a distinct solid–liquid phase separation. The equilibrium solution pH values for all the samples were noted. The manure solid fractions were collected by vacuum filtration employing regular Whatman filter paper (Grade I). Manure solids without any treatment derived after freeze drying are referred to as 'FDSM' henceforth, and manure solids derived after solid–liquid separation are termed as (a) manure solids with 0.15 M $FeCl_3$ (MSWF), (b) manure solids with control biochar (MSCB), and (c) manure solids with iron biochar (MSIB), respectively. The manure solids were dried at 40 °C for 36 h and were ground into powder form to achieve a uniform size (≈0.84 mm) using a ball mill (Retsch, PA, USA), operated for 10 min. The manure liquid fractions were stored in Nalgene plastic bottles at 4 °C until NH_4^+–N was determined colorimetrically.[4]

The other part of the materials and methods section is provided in the supporting information.

3 Results and discussion

3.1. Physicochemical characteristics of swine manure

The physicochemical properties of swine manure are provided in Table 1. The pH of the swine manure was alkaline (pH > 8). Gravimetric analysis revealed that the moisture content was 95.4%. The ultimate analysis included carbon (36.9%), nitrogen (3.88%), and hydrogen (5.68%). The NH_4^+–N and *ortho*-P concentrations in swine manure were recorded as 5487 mg L^{-1} and 388 mg L^{-1}, respectively. The total manure solids were 46.3 g kg^{-1}, and the solid content of manure includes oxygen, alkali, and alkaline earth metals in addition to C, H, N, S, and P. This study's scope is restricted; thus, it does not provide information related to other essential and optional components that contribute to the overall solid content of swine manure.

3.2. Importance of biochar for solid–liquid separation

We utilized different treatments for solid–liquid separation, as mentioned in the materials and methods section, including biochar (CB and IB) and without biochar, to evaluate the applicability of biochar for effective separation (Fig. S1). The effectiveness of the solid–liquid separation process depends on how well nutrients can be stabilized in the separate phases.[25] The manure liquid fractions derived after different treatments were analyzed for P (total P) concentration. We detected P in the liquid fractions derived after $FeCl_3$ treatment (without biochar) and $FeCl_3$ with CB, which were 23.63 mg L^{-1} (5.43% of total P) and 5.52 mg L^{-1} (2.27% of total P), respectively. $FeCl_3$ with IB treatment had 0 mg L^{-1} in its manure liquid fraction, which indicates that P remained in the solid fraction (100% P in the solid fraction). The probable reason could be the aggregation of negatively charged colloidal particles using IB, followed by the addition of 0.15 M $FeCl_3$, resulting in flocs first, and settling under gravity.5 The change in the standard state Gibbs' free energy (ΔG^0) is an important parameter for understanding the spontaneity and feasibility of the P separation process. We evaluated the ΔG^0 values of P for all three treatments, and the values were −16.4 kJ mol^{-1}, −18.2 kJ mol^{-1}, and −23.3 kJ mol^{-1} for manure liquid fractions after 0.15 M $FeCl_3$, 0.15 M $FeCl_3$ with CB, and 0.15 M $FeCl_3$ with IB, respectively. Biochar derived from wheat straw and modified with Fe also showed negative ΔG^0 values of −17.6 kJ mol^{-1}, −18.7 kJ mol^{-1}, and −19.9 kJ mol^{-1} at 10 °C, 25 °C, and 40 °C, respectively.[26]

Based on these results, we noticed that the ΔG^0 value was more negative for manure treated with 0.15 M $FeCl_3$ with IB for P, showing that this treatment was thermodynamically more favorable and the separation of P was more spontaneous and exothermic in nature. Therefore, the addition of IB is necessary for the separation of P into the solid fraction of swine manure during solid–liquid separation.

Table 1 Physicochemical properties of the swine manure used in this study

Parameters	Values[a]
pH	8.11 ± 0.01
Moisture (%)	95.4 ± 0.14
C (dry basis %)	36.9 ± 0.17
N (dry basis %)	3.88 ± 0.06
H (dry basis %)	5.68 ± 0.06
S (dry basis %)	0.0005 ± 0.008
NH_4^+–N (mg L^{-1})	5487 ± 93
Ortho-P (mg L^{-1})	388 ± 18
Total solids (g kg^{-1})	46.3 ± 0.14

[a] Results are the means of triplicates ± standard deviation.

3.3. The influence of different manure solids on the conductometric analysis

Conductometric analysis was carried out with varied manure solids after $FeCl_3$ treatment to understand the dispersive pattern of the cations associated with cation bridging between MC and P^- (*i.e.*, $H_2PO_4^-$ and HPO_4^{2-}, which are the dominant forms of P in the 2.12–12.67 pH range). The extent of cation dispersion depends on how the cations (Ca, Mg, and Fe) can move into a dispersive medium. We utilized 0.15 M NaCl as a dispersing medium to assess the cation's release pattern. This addition of Na will disperse the cations involved in cation bridging, reduce the Na concentration, and increase the concentration of other cations (Ca, Mg, and Fe). This conductometric analysis includes solution pH, ZP, and IS.

Surface charge is the primary determinant of colloidal particle stability and is influenced by both solution pH and IS. The solution pH of FDSM varied from 7 to 7.5 with the volume (0–30 mL) of the 0.15 M NaCl solution. The solution pH of other manure solids (MSWF, MSCB, and MSIB) ranged from 4 to 5 and it decreased further after the 0.15 M $FeCl_3$ treatment due to the hydrolysis of $FeCl_3$, which produced protons (Fig. 1a). We observed that MSIB had the lowest solution pH among the solids at 0 mL of NaCl solution; this could be due to the IB, which releases protons during the hydrolysis of Fe^{+3} ions.[5]

Fig. 1b shows that the particles of the investigated suspensions are negatively charged, and the ZP of FDSM ranged from −20 mV to −16 mV over the entire volume of 0.15 M NaCl (0 to 30 mL). The negative ZP values indicate the inadequate destabilization of colloidal particles of swine manure.[27] As previously reported, the negatively charged surface of swine manure particles is primarily attributed to the abundance of ionizable functional groups, including carboxylic, phenolic, and aldehyde groups.[20,28] The manure solids (MSWF, MSCB, and MSIB) had positive surface charges varying from 3.4 to 21.8 mV. The presence of positively charged surface ions (Fe^{3+}, Ca^{2+}, and Mg^{2+}) on manure solids indicates electrostatic repulsion among the particles themselves. However, these positively charged particles can interact with negatively charged particles (clay minerals, humic acid, and colloidal P^-). A higher ZP leads to stronger repulsion between the colloidal particles, resulting in slower aggregation and can cause sedimentation.[29]

The IS of different manure solids under the influence of NaCl is presented in Fig. 1c. At a low volume (0 mL) of NaCl, the lowest IS

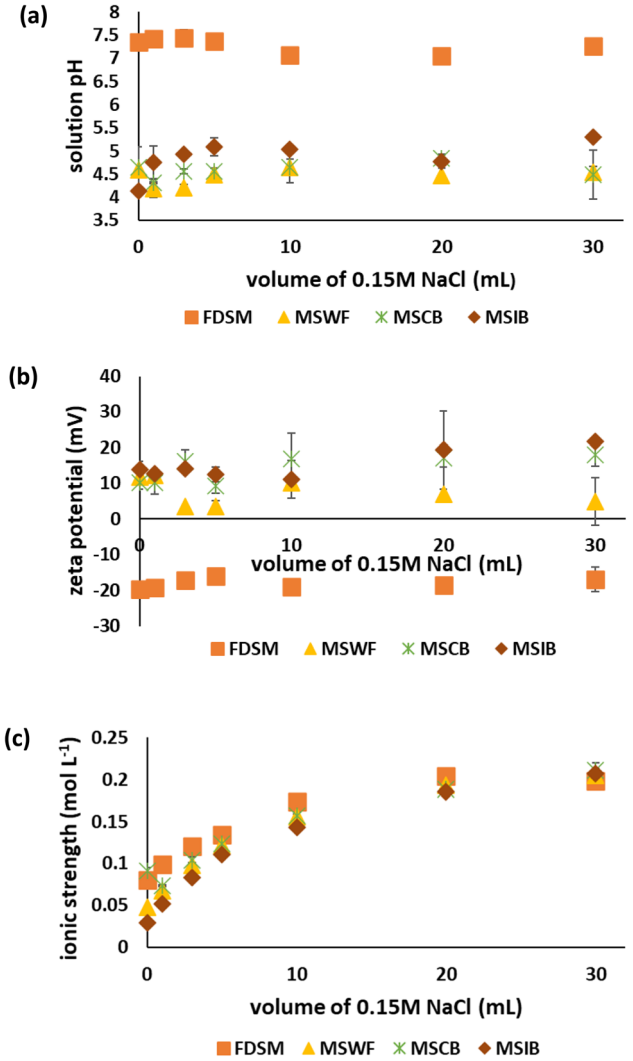

Fig. 1 Effect of dispersing medium (0.15 M NaCl) on the solution pH (a) zeta potential, (b) and ionic strength, and (c) of swine manure (FDSM) and manure solids (MSWF, MSCB, and MSIB) derived after treatment with 0.15 M $FeCl_3$. Experimental conditions: FDSM-freeze-dried swine manure, MSWF-manure solid with $FeCl_3$, MSCB-manure solid with control biochar, MSIB-manure solid with iron biochar; 0.1 g of manure solids mixed with 10 mL of deionized water, followed by the addition of 0 to 30 mL of 0.15 M NaCl solution. Error bars represent the standard deviation of the sample size ($n = 3$). Error bars that are not visible are smaller than the symbol.

was recorded for MSIB (0.03 mol L^{-1}) and the highest was documented for MSCB (0.09 mol L^{-1}), followed by FDSM (0.08 mol L^{-1}), and MSWF (0.05 mol L^{-1}). As the 0.15 M NaCl solution volume increased, the respective solution's IS also increased because of the high dissociation ability of NaCl, resulting in more Na^+ and Cl^- ions in the solution. We noticed that the IS for MSIB remained low compared to the others (FDSM, MSWF, and MSCB) until NaCl (20 mL) was added. We suspect that NaCl's dispersive effect could not completely disperse the cations associated with cation-bridging, resulting in low numbers of dissociated ions and, therefore, a low IS was observed. However, for FDSM over a range of NaCl volumes (0–20 mL), NaCl showed a significant dispersive effect, resulting in high IS.

Raman spectra of different manure solids under the influence of different volumes of dispersing medium (NaCl, 0–30 mL) are presented in Fig. S2. Two noticeable peaks were identified at 1580 cm^{-1} (G-band) and 1350–1380 cm^{-1} (D-band) in all samples (FDSM, MSWF, MSCB, and MSIB), referring to the graphitic (E_2g vibrational mode of sp^2-C) and disordered carbon structure (A_1g symmetry breathing modes in disordered sp^2-C), respectively.[30] All types of manure solids showed an increase in the Raman spectra intensity, especially at the G and D bands, after 30 mL of NaCl solution was added. However, there was a significant increment in the peak intensity of G- and D-bands of MSCB and MSIB samples (Fig. S2c and S2d). This was probably due to electrostatic stability and better dispersion of colloidal particles by NaCl solution, which decreases agglomeration and enhances the surface exposure of active carbon.[31] This phenomenon is particularly important for C-rich environments (MSCB and MSIB), where the structural characteristics of pyrolyzed carbon become more evident under high IS conditions.

Similarly, the change in surface functionality of all the manure solids under the dispersing medium (0.15 M NaCl) was evaluated based on the FTIR analysis. The FTIR spectra for all the manure solids are presented in Fig. S3 and S4. These FTIR spectra can be divided into three regions where the maximum change occurred. The first region, where peaks appeared at wavenumbers ranging from 3400 cm^{-1} to 3100 cm^{-1}, corresponds to O–H/N–H/≡C–H (sp-C) stretching. The second region is attributed to aliphatic –C–H stretching (2920 cm^{-1} to 2848 cm^{-1}), the peak at 2920 cm^{-1} is mainly ascribed to asymmetric stretching of the $-CH_2$ (sp^2-C) group, and the peak at 2848 cm^{-1} resulted from symmetric stretching of the $-CH_3$ (sp^3-C) group. The third region (1700 cm^{-1} to 1400 cm^{-1}) showed a maximum change in the spectra. For FDSM, without any dispersing medium, the peaks appeared at 1556 cm^{-1} and 1530 cm^{-1}, corresponding to $-CONH_2-$ (sp^2-C) stretching and secondary aromatic amines (–NH–), respectively (Fig S3a). With different volumes of dispersing medium (0–30 mL, NaCl), several new peaks appeared at 1650 cm^{-1} (–C═O, amide-I), 1627 cm^{-1} (–C═O, amide-II), and 1574 to 1538 cm^{-1} (–NH–). Higher relative % transmission peaks of all three zones for each manure solid were probably due to enhanced IS and dispersion with NaCl addition.[32] We anticipate that high dispersion leads to the disturbance of the cation bridging mechanism between the active cations (Ca, Mg, and Fe) present in manure with the C═O group of manure colloids.[33] A similar pattern was also observed for other manure solids (MSWF, MSCB, and MSIB), as presented in Fig. S3b and S4. Based on the above results, the dispersing medium (0.15 M NaCl solution) significantly influenced the solution pH, ZP, and IS, providing a better understanding of colloidal stability, dispersive behavior, and nutrient mobility.

3.4. Influence of different manure solids on the pH metric analysis

The manure solids (FDSM, MSWF, MSCB, and MSIB) were subjected to a pH metric titration curve to comprehend the complex relationship between the coagulant (0.15 M $FeCl_3$) and the organic matrix of swine manure. The characteristics of

manure solids depend on the nature of the active functional groups and how they are associated with other molecules.[11–13] With the aid of pH metric titration, we have compared the MC characteristics derived after different treatments and obtained important insights about coordination bridging and metal cation bridging. The pH metric titration analysis includes the solution pH, ZP, and IS of manure solids, as presented in Fig. 2 and 3. The solution pH for all the manure solids showed a decreasing trend as the milliequivalent of acid (0.1 M HCl) increased due to the increased proton concentration in the solution (Fig. 2a). In contrast, the solution pH for manure solids increased as the milliequivalent base (0.1 M KOH) increased due to the decreased concentration of protons in the solution (Fig. 2b). It is worth noting that at 0 milliequivalent of acid/base, the highest solution pH was recorded for FDSM because it was not exposed to $FeCl_3$.

The ISs of different manure solids under the influence of milliequivalents of acid (0.1 M HCl) and base (0.1 M KOH) are presented in Fig. 2c and d. This indicates that the IS of FDSM at 0 milliequivalent of acid (0.1 M HCl) was the highest (0.18 mol L^{-1}); as the milliequivalent of acid increased, the IS of FDSM decreased (0.15 mol L^{-1}), which indicates that some of the ions moved to the solid phase. Contrary to FDSM, manure solids (MSWF, MSCB, and MSIB) showed a successive increase in IS with an increase in milliequivalent acid. This confirmed that most ions go into the liquid phase from the solid phase of manure solids.

The ZP of FDSM as a function of pH ranged from −6 mV to −27 mV at pH 2 to 12 (Fig. 3a). In contrast, those of MSWB, MSCB, and MSIB ranged from −42 mV to 33 mV, −34 mV to 27 mV, and −35 mV to 23 mV, respectively, at pH values varying from 2 to 10 (Fig. 3). For FDSM, the ZP was negative throughout the pH range due to the abundance of many organic compounds rich in oxygenated functional groups. Deprotonation of surface-bound carboxylic groups started as the solution pH increased.[34] With base addition, the pH of the suspension increased, resulting in a negative ZP, and the particles acquired a more negative charge.[35] On the contrary, other manure solids (MSWB, MSCB, and MSIB) reported a positive surface charge at a lower pH value (<5.5) and a negative charge at a higher pH value (>5.5). The point where both positive and negative charges became zero is considered the point of zero charge (pH_{pzc}), which was 6.08, 5.96, and 5.81 for MSWB, MSCB, and MSIB, respectively (Fig. 3b–d). This indicates that the addition of $FeCl_3$ as a coagulant resulted in more positive values of ZP for manure solids, and the reason might be the electrostatic attraction binding between the positively charged iron and negatively charged manure colloids. The higher charge density of iron induced a more positive charge on the manure colloids at lower pH. The lowest pH_{pzc} (5.81) for MSIB was mainly due to several reactions: iron hydrolysis, followed by hydration of iron oxide, and proton donation.[5]

Similar to conductometric analysis, the FTIR spectra of all the manure solids (MSWF, MSCB, and MSIB) with FDSM can be divided into three regions (Fig. S5 and S6). The maximum change appeared in regions two (2920–2848 cm^{-1}) and three (1700–1400 cm^{-1}), which correspond to aliphatic –C–H and –$CONH_2$– stretching at 1660–1620 cm^{-1}, –NH– at 1540 cm^{-1}, and carbonate at 1460 cm^{-1}. There was an increase in the

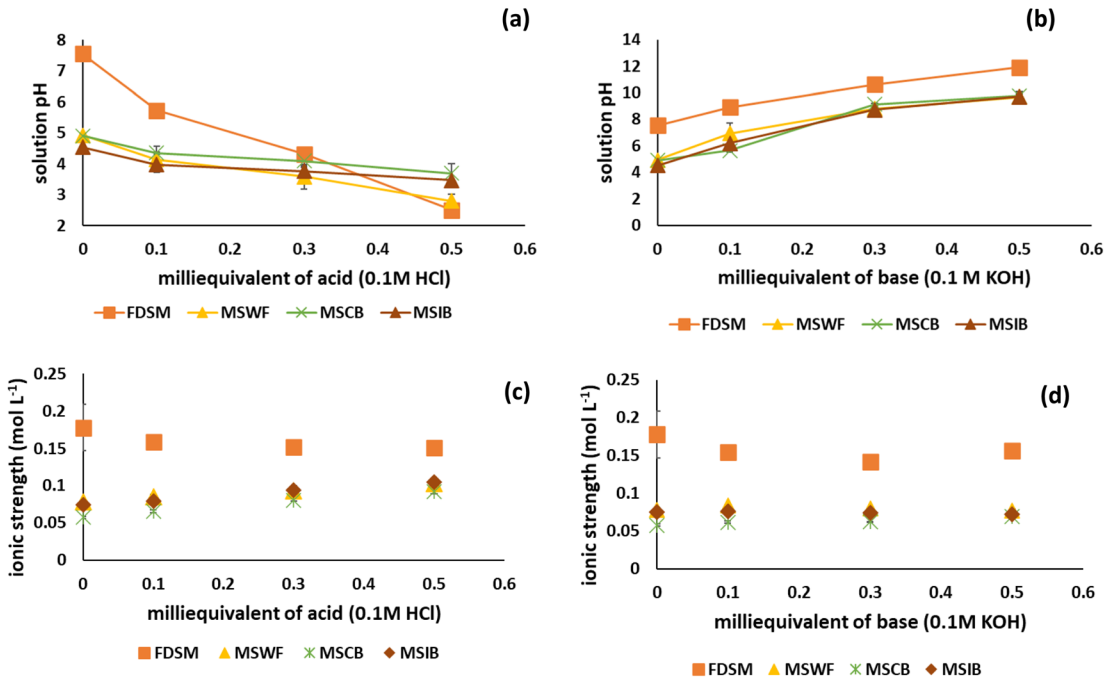

Fig. 2 pH metric curve analysis: (a) and (b) solution pH, (c) and (d) ionic strength of the solution as a result of the addition of different milliequivalents of acid (0.1 M HCl) and base (0.1 M KOH). Experimental conditions: FDSM-freeze-dried swine manure, MSWF-manure solids with $FeCl_3$, MSCB-manure solids with control biochar, MSIB-manure solids with iron biochar; 0.1 g of manure solids mixed with 10 mL of 0.05 M NaCl solution, followed by the addition of 0 to 5 mL of 0.1 M HCl/0.1 M KOH to reach the targeted pH values of 2 to 12. Error bars represent the standard deviation of a sample size ($n = 3$). Error bars that are not visible are smaller than the symbol.

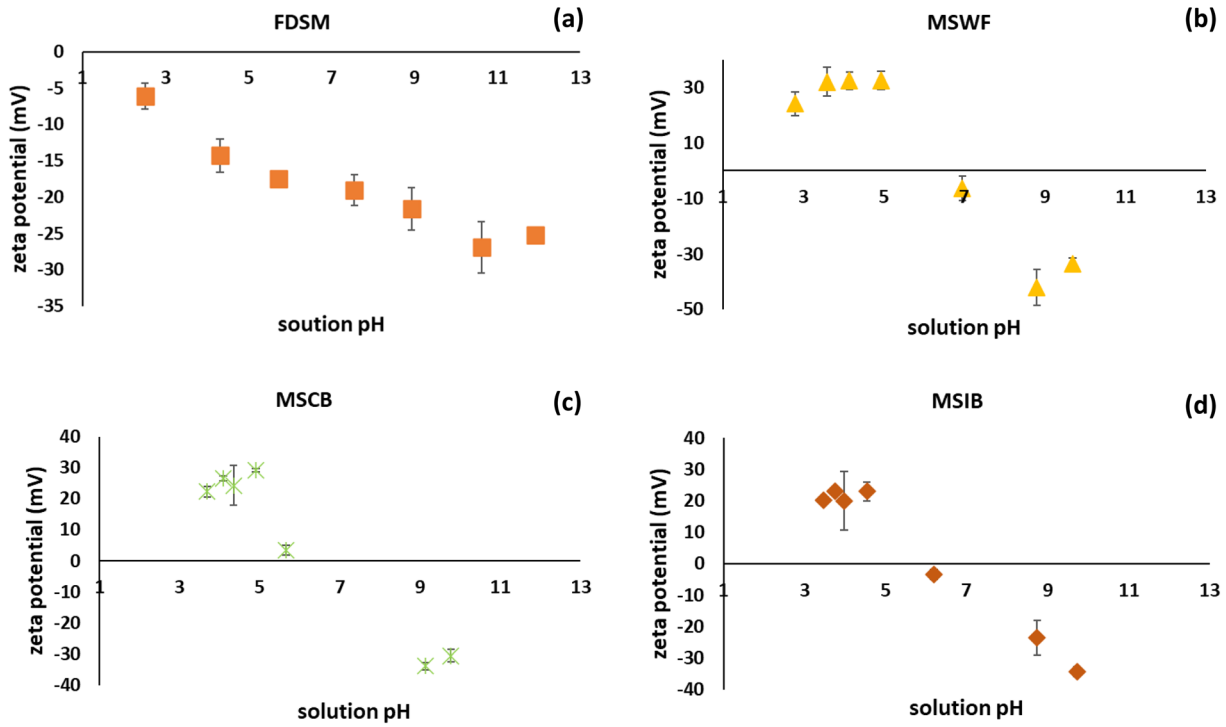

Fig. 3 Zeta potentials of different manure solids: (a) FDSM, (b) MSWF, (c) MSCB, and (d) MSIB under the influence of different solution pH values. Experimental conditions: FDSM-freeze-dried swine manure, MSWF-manure solid with $FeCl_3$, MSCB-manure solid with control biochar, MSIB-manure solid with iron biochar; 0.1 g of manure solids mixed with 10 mL of 0.05 M NaCl solution, followed by the addition of 0 to 5 mL of 0.1 M HCl/0.1 M KOH to reach the targeted pH values of 2 to 12. Error bars represent the standard deviation of a sample size ($n = 3$). Error bars that are not visible are smaller than the symbol.

relative percentage transmittance with an increase in the volume of 0.1 M HCl or 0.1 M KOH (from 0 to 5 mL) in both regions. The reason could be the exposure of aliphatic chains, likely due to the disruption of H-bonds and the dissociation of active cations (Ca, Mg, and Fe) bound with functional groups such as –C═O, –NH–, and –COO, respectively.[5,33] However, FTIR spectra for FDSM decreased at high volume of acid (5 mL of 0.1 M HCl), potentially due to solubilization of organic colloids (Fig. S5a). FTIR spectra of MSCB and MSIB were also recorded, showing an increase in the spectral intensity with increasing volumes of acid (0.1 M HCl) and base (0.1 M KOH). Notably, carbonate peaks at 1460 cm^{-1} disappeared after 0.1 M HCl (5 mL) treatment because carbonates were converted to carbon dioxide under the acidic environment (Fig. S6). However, carbonate peaks remained at 1460 cm^{-1} even after 0.1 M KOH treatment, indicating the stability of carbonates under alkaline conditions, forming insoluble carbonates ($CaCO_3$, $FeCO_3$). Based on the above results, we found that coordination and cation bridging changed significantly under the influence of varied solution pH, which resulted in different ZPs and ISs for FDSM and different manure solids.

3.5. Influence of different manure solids on the Mehlich-III (M-III) extraction

With the Mehlich-III (henceforth denoted as 'M-III') extractant, we tried to break the ligand bridging in different manure solids (FDSM, MSWF, MSCB, and MSIB). We suspected that P^- present in different manure solids was bound through cation-bridging and ligand-bridging, where P^- ($H_2PO_4^-$ and HPO_4^{2-}) is bonded to two metal ions at once. The detailed characterization was done using different analyses, such as solution pH, ZP, and IS, under the influence of different volumes of M-III solution (0–12 mL). The solution pH values of the different manure solids are presented in Fig. S7a, and a decreasing trend is reported for all the manure solids with an increase in the volume of M-III solution. An increase in the M-III solution volume resulted in a high proton (H^+) release from acids (acetic acid and HNO_3), reducing the solution pH. On comparing the solution pH at 0 (FDSM > MSCB > MSIB > MSWF) and 12 mL (MSWF > MSIB > FDSM > MSCB) volume addition of M-III solution, we noticed completely different trends. At high M-III volume, MSWF had the highest solution pH due to acid saturation, and the solution started acting as a buffered solution.

The particle surface charge of different manure solids (FDSM, MSWF, MSCB, and MSIB) was investigated using ZP. FDSM exhibited ZP values varying from −16 mV to −4.85 mV at different volumes of M-III solution (0–12 mL). However, the ZP for the other manure solids varied from 20 mV to −4.13 mV for MSWF, 23.22 mV to −1.71 mV for MSCB, and 17.81 mV to −0.13 mV for MSIB, respectively (Fig. S7b). We noticed a negative ZP for MSWF, MSCB, and MSIB at the M-III volume (>6 mL). The probable reasons might be the desorption of metal cations, deprotonation of functional groups, such as carboxylic (–COOH) and phenolic (–OH), and weakening ligand bridging, resulting in more negatively charged ions.[34]

The ISs of different manure solids (FDSM, MSWF, MSCB, and MSIB) with different volumes of M-III (0–12 mL) are presented in Fig. S7c. The trend was similar to that of the conductometric curve; as the volume of M-III increased, the IS of various manure solids also increased. For FDSM, the IS was found to be maximum at 0 mL (0.19 mol L^{-1}) and 12 mL (0.35 mol L^{-1}) of M-III solution. In contrast, the lowest values of IS were recorded for MSIB at 0 mL (0.12 mol L^{-1}) and 12 mL (0.33 mol L^{-1}) of M-III solution. The probable reason for increased IS at high M-III volume (12 mL) might be ionic dissociation and higher total ion concentration. These results indicate that M-III with dispersing medium (0.05 M NaCl) solution successfully influenced the solution pH, ZP, and IS, confirming the mobility and stability of the active cations and ligands from the solid phase to the liquid phase.

3.6. Comparison of different extractants

The chemical constituents of the stabilizing agents and the extractant employed greatly impact the nutrient extractability. Herein, we utilized different extractants, such as M-III, Olsen, and citrate-bicarbonate-dithionite (CBD), to evaluate the release of macronutrients (Ca, Fe, Mg, K, and P) from FDSM and other manure solids (MSWF, MSCB, and MSIB).

3.6.1. Effect of M-III extraction on the release of macronutrients. Different manure solids (FDSM, MSWF, MSCB, and MSIB) showed significantly different macronutrient release patterns under M-III extraction solution (Fig. 4a). Among all the treatments, FDSM showed the highest release of K (113 884 mg kg^{-1}), which was substantially higher than other treatments. This elevated K release was expected, as K in the raw swine manure exists primarily in soluble or exchangeable forms that M-III can easily extract. However, the release of K was significantly reduced in MSWF, MSCB, and MSIB, suggesting that most of the K exists in the liquid fraction,[5] and the remaining K of the solid fraction was stabilized with biochar during $FeCl_3$ treatment.

The lowest amount of Fe was extracted from FDSM (1564 mg kg^{-1}), and the highest amount of Fe was extracted from MSWF (60 625 mg kg^{-1}) and remained elevated in MSCB (60 284 mg kg^{-1}) and MSIB (60 300 mg kg^{-1}). The increased availability of Fe might be due to the formation of Fe-rich complexes that remained partially extractable by acidic M-III solution. Notably, Ca and Mg levels were comparatively low in all samples, with minor reductions following $FeCl_3$ treatment, likely due to the replacement or masking of exchangeable Ca^{2+}/Mg^{2+} by Fe^{3+} ions.

In FDSM, P release was modest (19 520 mg kg^{-1}), but in MSWF (222 mg kg^{-1}), MSCB (224 mg kg^{-1}), and MSIB (202 mg kg^{-1}), it was significantly lower. The formation of Fe–P complexes during coagulation, and the improved sorption onto biochar surfaces, especially in MSIB, where iron-modified biochar probably supplied more binding sites, are responsible for this reduction, as presented in eqn (i)–(iv).

$$\sim R\text{–}COO\cdots M^{n+}\cdots H_2PO_4 + H^+ \rightarrow \sim R\text{–}COOH + H_2PO_4^- + M^{n+} \quad \text{(i)}$$

(cation-bridged P^-)

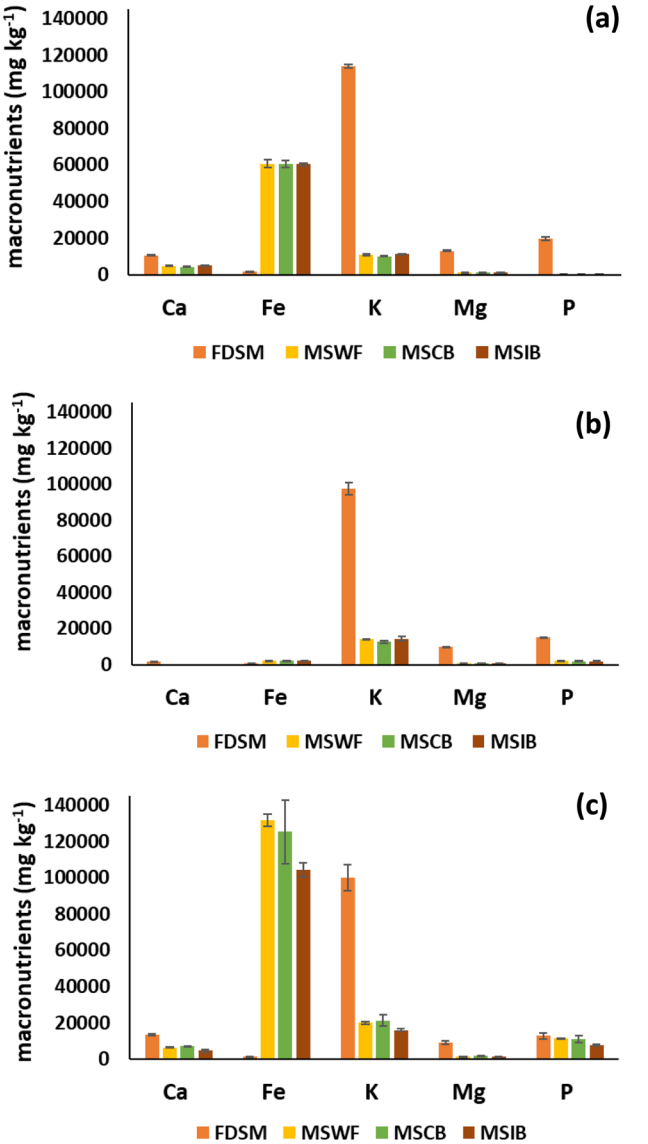

Fig. 4 Comparison of the release pattern of macronutrients (Ca, Fe, Mg, K, and P) under the influence of different extractants: (a) M-III, (b) Olsen, and (c) CBD. (FDSM-freeze-dried swine manure, MSWF-manure solid with $FeCl_3$, MSCB-manure solid with control biochar, MSIB-manure solid with iron biochar). Error bars represent the standard deviation of a sample size ($n = 3$).

$$\sim R\text{–}COOH + H_2PO_4^- + M^{n+} + EDTA^{4-} \rightarrow \sim R\text{–}COOH + H_2PO_4^- + [M - EDTA]^{(n-4)-} \quad \text{(ii)}$$

$$3H_2PO_4^- + Fe^{3+}(*) \rightarrow [Fe(H_2PO_4)_3]\ \text{(reprecipitated)} \quad \text{(iii)}$$

* (The release of free Fe might be from cation-bridging or Fe-oxides of the biochar surface)

$$Fe\text{–}P + EDTA^{4-} + H^+ \rightarrow \text{no reaction} \quad \text{(iv)}$$

(Fe–P, strong inner-sphere complexes).

The reactions presented in eqn (i)–(iv) indicate that P ($H_2PO_4^-$ is the dominant form of P at pH 2.5–6.5), which is

cation-bridged and is susceptible to M-III extraction. The release of free Fe without P indicates the selective mobilization of Fe, possibly from Fe-organic matter complexes or Fe-oxides on the biochar surface. We noticed a secondary reaction, where this free Fe was reprecipitated with P^- due to a change in the solution pH. The Fe solubility decreased with an increase in solution pH, and the activity of $H_2PO_4^-$ was very low at pH 2, which means it released some of the P, but it was reprecipitated into the solid phase and determined as low P.[36] We found only ~1.4% of total Fe, which again confirmed the low solubility of Fe. On the contrary, M-III was ineffective at liberating P from inner sphere Fe–P complexes; thus, very little P was extracted from MSIB (only 1% P from FDSM). These interactions rendered P less extractable, suggesting a possible trade-off between plant availability and nutrient retention.

3.6.2. Influence of Olsen extraction on the release of macronutrients. The Olsen extraction method is primarily designed to estimate plant-available P in calcareous soil by desorbing loosely bound *ortho*-P^- ions through carbonate-induced replacement reactions.[37] The macronutrient release profile using the Olsen extraction solution showed clear variation among all treatments (FDSM, MSWF, MSCB, and MSIB) (Fig. 4b). Among the macronutrients analyzed, K has the highest extractable concentration in FDSM (97 551 mg kg^{-1}), followed by MSIB (14 349 mg kg^{-1}), MSWF (14 028 mg kg^{-1}), and MSCB (12 564 mg kg^{-1}), respectively. The possible reason for the highest extractable K concentration in FDSM is its high solubility, poor binding, and the exchangeable nature of K in manure.[38]

A similar pattern was seen in P extractability, with FDSM exhibiting noticeably greater P (14 964 mg kg^{-1}) than other samples treated with $FeCl_3$ and biochar; the P concentrations were 2033 mg kg^{-1}, 1959 mg kg^{-1}, and 1933 mg kg^{-1} for MSWF, MSCB, and MSIB, respectively. The formation of poorly soluble Fe–P complexes during coagulation is known to resist desorption in $NaHCO_3$ solution and is responsible for the notable decrease in P availability in MSWF, MSCB, and MSIB, respectively.[39] The additional P immobilization in MSIB is the result of the combined effect of Fe-enhanced sorption sites and ligand exchange mechanisms facilitated by the iron-modified biochar surface,[40] as presented in eqn (v)–(ix).

$$NaHCO_3 \rightarrow Na^+ + HCO_3^- \quad \text{(v)}$$

$$Ca^{2+} + HCO_3^- \rightarrow CaCO_3 + H^+ \quad \text{(vi)}$$

$$Ca_5(HPO_4)_3(OH) + 4HCO_3^- \rightarrow 5Ca^{2+} + 3HPO_4^{2-} + 4CO_2 + 6OH^- \quad \text{(vii)}$$

$$\sim R\text{–}COO\cdots M^{n+}\cdots H_2PO_4 + 2HCO_3^- \rightarrow \sim R\text{–}COO^- + M_2(CO_3)_n + H_2PO_4^- + 2H^+ \quad \text{(viii)}$$

$$Fe - P^*/FePO_4^{**} + NaHCO_3 \rightarrow Fe \text{ remains insoluble} \quad \text{(ix)}$$

(*inner sphere complex and ** mineral phase).

The presence of HCO_3^- from $NaHCO_3$ promotes the precipitation of $CaCO_3$, which lowers the Ca concentration in the solution and prevents precipitation as Ca–P.[41] We observed a change in the solution pH after Olsen extraction, which is responsible for the increased solubility of P from the Ca–P mineral and the breaking of cation-bridged P^-, as presented in eqn (v)–(ix). However, Diaz *et al.*[42] found that increased Ca concentration and alkaline pH led to a sharp decline in P solubility. Moreover, the inner sphere complex (iron (oxy) hydroxide bound P^-) remained insoluble. The extractability of Ca, Mg, and Fe remained minimal for all manure solids (FDSM, MSWF, MSCB, and MSIB). The Olsen solution was not developed to dissolve multivalent cations or their oxides. Lower concentrations of Fe were present in the extracts from MSWF (2127 mg kg^{-1}), MSCB (2062 mg kg^{-1}), and MSIB (2213 mg kg^{-1}), respectively. This further confirmed the formation of stable $Fe(OH)_3$ precipitates and Fe-organic complexes during coagulation, which are primarily insoluble in bicarbonate systems.[43] These findings were supported by the XRD characterization results.

XRD analysis was conducted to evaluate the dominance of the inorganic mineral phase in MSIB before and after Olsen extraction, as presented in Fig. S8. The XRD spectra of MSIB before Olsen extraction exhibited the dominance of quartz at two-theta values of 20.85, 26.65, and 50.14, respectively. The calcite and sylvite peaks were recorded at two-theta values of 29.40, 43.14 and 28.35, and 40.53, respectively. Our previous XRD results for IB showed the dominance of hematite and magnetite mineral phases, indicating the oxidation of Fe^{2+} to Fe^{3+} during the drying of $FeSO_4$-treated biomass.[23] The Fe-oxides present in the IB provide ferrol sites for P^- by forming an inner sphere complex, while $FeCl_3$ treatment was responsible for Fe hydrolysis, resulting in hydrated Fe-oxides followed by P^- stabilization on amorphous Fe surfaces. The XRD results also confirmed the presence of P-based minerals such as hydroxyapatite and strengite at two-theta values of 32.19 and 39.90, and 28.64 and 16.07, respectively. After the Olsen extraction, hydroxyapatite peaks disappeared, and strengite peaks remained the same as before the extraction, confirming the release of P from hydroxyapatite, whereas the Olsen solution was not able to dissolve Fe–P from strengite. This finding was supported by SEM-EDS results, as presented in Fig. S9–S11. This SEM-EDS mapping of three particles of MSIB indicated that P is mostly associated with Fe. This association did not change much, even after the Olsen treatment, indicating that Fe and P are closely associated.

All the above findings suggest that Olsen extraction was responsible for increased P solubility from Ca–P minerals by promoting $CaCO_3$ precipitation, which in turn reduced the Ca concentration in the solution. On the contrary, the Olsen extractant was proved ineffective for Fe–P complexes, as the solution pH change induced by HCO_3^- was insufficient to disrupt the strong Fe–P association.

3.6.3. Impact of CBD extraction on the release of macronutrients. Citrate-bicarbonate-dithionite (CBD) is a strong reductive extractant that promotes ligand dissolution and reductively mobilizes metal-P^- complexes to solubilize iron oxide and liberate occluded P from Fe–P.[44] After CBD extraction, the highest Fe concentration was observed for MSWF (131

552 mg kg^{-1}), followed by MSCB (125 280 mg kg^{-1}), and MSIB (104 468 mg kg^{-1}), respectively (Fig. 4c). The high level of Fe mobilization in MSWF was in line with the previous use of $FeCl_3$, which most likely produced amorphous $Fe(OH)_3$ or Fe-organic complexes that were easily reducible in CBD conditions. The addition of biochar might have fixed some of the Fe by surface complexation or sorption processes, which decreased the Fe release in MSCB (~5%) and MSIB (~21%) compared to MSWF. The drastic reduction of Fe (21%) in MSIB confirmed that Fe was still present in a reactive, reducible form.

For FDSM, K release was recorded as the highest (99 958 mg kg^{-1}), indicating its highly soluble and exchangeable nature. Conversely, K availability was greatly reduced by $FeCl_3$ treatment (MSWF (19 895 mg kg^{-1})) and subsequent biochar incorporation (MSCB (21 264 mg kg^{-1}) and MSIB (15 823 mg kg^{-1})). The observed decrease in K availability indicates the physical and chemical stabilization of soluble K. Under the influence of CBD, which is non-acidic and reductive, there was no effective disruption of this stablized K was observed.

Moderate levels of Ca and Mg were released by CBD extraction in all manure solids; however, FDSM showed higher concentrations of Ca (13 325 mg kg^{-1}) and Mg (9062 mg kg^{-1}). The manure solids after $FeCl_3$ treatment showed decreased extractability, increasing the possibility of retention on biochar exchange sites or co-precipitation with different Fe phases. CBD mainly targets the reducible Fe-bound fraction, and its impact on alkaline earth metals is secondary and mostly reliant on initial solubility rather than particular complexation.[43]

With CBD extraction, we were able to extract more P from FDSM (12 680 mg kg^{-1}), and from other manure solids, which were 11 294 mg kg^{-1}, 11 165 mg kg^{-1}, and 7477 mg kg^{-1} for MSWF, MSCB, and MSIB, respectively. The P present in FDSM was easily extracted due to its readily extractable organic and inorganic forms. However, MSWF and MSCB solids showed less extraction of P (10–12%) compared to FDSM; for MSIB, a 41% reduction of P extraction was observed. Interestingly, the lower P release from MSIB than MSCB indicates that iron-modified biochar contributed to Fe stabilization and improved ligand exchange surfaces, which were not easy to break.[10] Under the influence of CBD extraction, cation-bridged P^- is easily extracted, but Fe–P complexes are challenging, and multiple steps are required to disrupt Fe–P bonds to release P, as presented in eqn (x)–(xiii). Firstly, hydrolysis of the inner sphere complex and mineral phase of Fe-bound P occurs, which is responsible for releasing Fe^{3+} and some P^-. Secondly, dithionite (SO_3^{2-}) reduces Fe^{3+} (mainly oxides and oxyhydroxide of Fe from biochar surfaces) to Fe^{2+}; this reduction destabilizes the Fe–P and $FePO_4$ lattice and releases soluble Fe^{2+} and $H_2PO_4^-/HPO_4^{2-}$ species depending on the solution pH. Thirdly, citrate stabilizes Fe^{2+} in solution and inhibits the reprecipitation of Fe–P or Fe–OH phases.

$$\sim R\text{–}COO\cdots M^{n+}\cdots H_2PO_4 + C_6H_5O_7^{3-} \rightarrow \sim R\text{–}COO^- + H_2PO_4^- + [M\text{–}C_6H_5O_7]^{(n-3)-} \quad (x)$$

$$Fe - P^*/FePO_4^{**} + OH^- \rightarrow Fe^{3+} - OH + H_2PO_4^-/HPO_4^{2-} \text{(depending on solution pH)} \quad (xi)$$

$$Fe^{3+} + e^- \rightarrow Fe^{2+} \text{ (reduced Fe by } Na_2S_2O_4) \quad (xii)$$

$$Fe^{2+} + C_6H_5O_7^{3-} \rightarrow [Fe^{2+}(C_6H_5O_7)]^- \text{ (chelated by citrate, prevents reprecipitation)} \quad (xiii)$$

FTIR spectra of FDSM, MSWF, MSCB, and MSIB after different extraction solutions (M-III, Olsen, and CBD) also confirmed the involvement of the different functional groups and their associations (Fig. 5). For all the samples, the peaks appearing between 3300–3400 cm^{-1} correspond to O–H/N–H/≡C–H stretching. Before any treatment (FDSM), the peak recorded at ~3271 cm^{-1} was narrower, but after $FeCl_3$ and biochar treatments, the broadening of peaks was observed, confirming the formation of a strong H bond and also indicating cation bridging and chelate complexes.[24] A small peak appeared at 2944 cm^{-1}, corresponding to P–OH stretching vibrations for different forms of PO_4–P present in FDSM and other manure solids (MSWF, MSCB, and MSIB). Asymmetric (~2920 cm^{-1}) and symmetric (~2850 cm^{-1}) stretching vibrations of aliphatic C–H appeared prominently in FDSM. However, the peak intensity was reduced after $FeCl_3$ (MSWF) and biochar treatments (MSCB and MSIB). These changes were almost constant among the different extractants (M-III, Olsen, and CBD) tested in this study. The influence of different extractants was observed in the range of 1700 cm^{-1} to 1400 cm^{-1}. For FDSM, the peaks appeared at 1700 cm^{-1}, 1680 cm^{-1}, 1630 cm^{-1}, and 1530 cm^{-1}, corresponding to amide (–C=O) stretching and secondary aromatic amines, respectively. However, for MSWF, MSCB, and MSIB, the intensity of these peaks was reduced, and some of them disappeared, while some new peaks appeared due to hydrolysis. Under the influence of M-III and Olsen extractants, amide peaks were not clearly visible, but after CBD extraction, amide peaks could be clearly seen. This indicates that the C=O group was involved in cation bridging and other complex compounds, which became free after the hydrolysis. This was the reason for the higher concentration of Fe and P after CBD extraction.

CBD destabilizes the cation-bridging structure, releasing both the organic ligand and P^-. CBD also dismantles firmly bound Fe–P and $FePO_4$ phases by activating phosphorus release through a combined process, including hydrolysis, reduction of Fe^{3+}, and chelation reactions. The strong electrostatic and covalent interactions involved in inner-sphere complexation are frequently too strong to be overcome by pH modification alone. CBD also highlights the enhanced nutrient recovery from organically stabilized manure solids, with a special emphasis on the significance of redox chemistry in P mobilization, particularly in the iron (oxy)hydroxide-rich environment.

3.7. Environmental implications

The findings of this study provide important insights into P dynamics in Fe-rich environments, highlighting the drawbacks of the traditional extractants and the vital function of the redox process in P mobilization. P was partially recovered from manure solids using M-III and Olsen extractants because persistent, stable Fe–P interactions limited the recovery

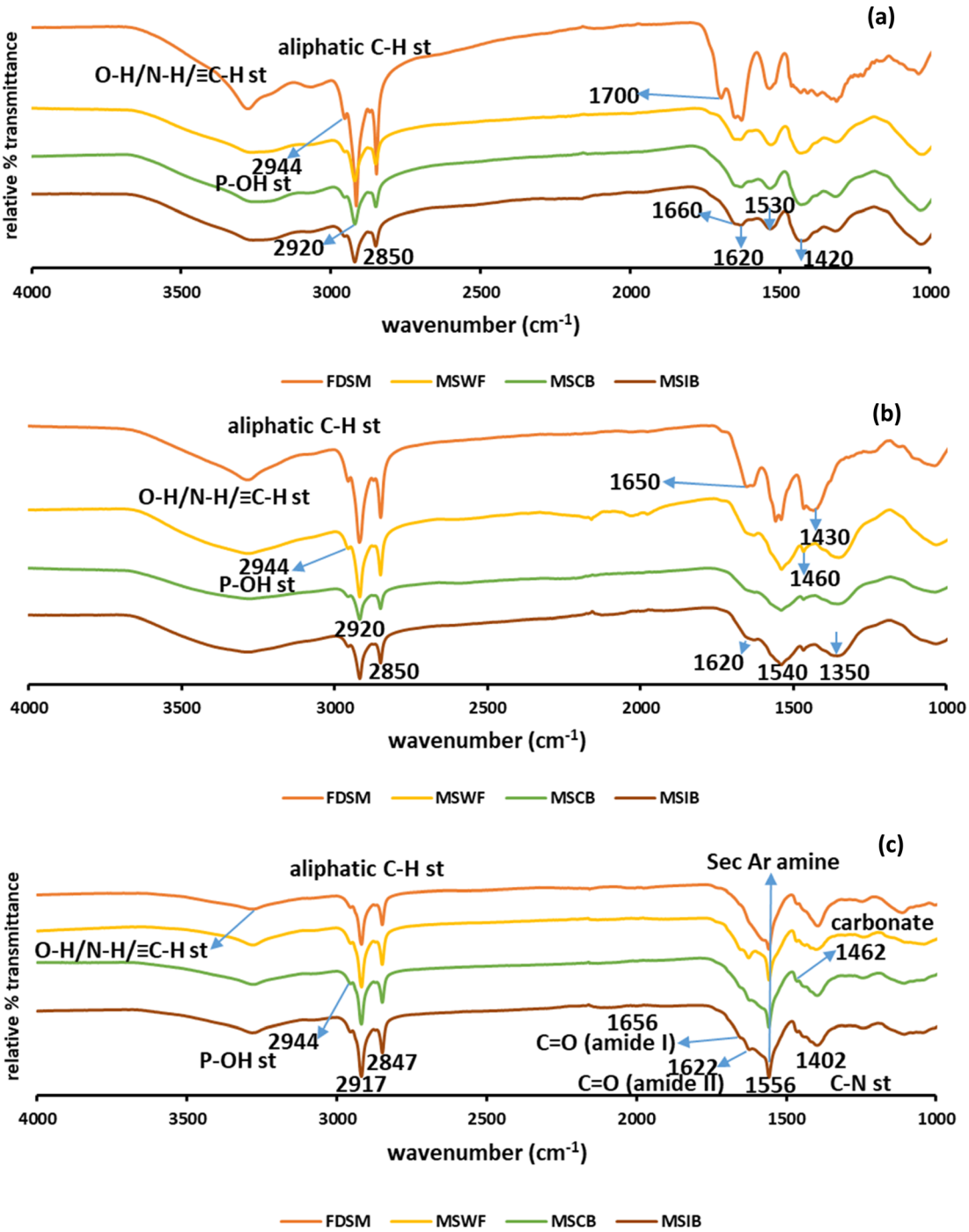

Fig. 5 Fourier transform infrared spectra of freeze-dried swine manure (FDSM) and manure solids (MSWF, MSCB, and MSIB) after the addition of different extractants: (a) M-III, (b) Olsen, and (c) CBD.

effectiveness. This behavior is typical of Fe-rich soils, where P is frequently trapped in crystalline or amorphous Fe (oxy) hydroxide phases, making it essentially unavailable to plants. Conversely, the CBD extractant demonstrated significantly better P release, which can be attributed to its ability to both chelate and reduce Fe^{3+}, facilitating the dissolution of Fe–P complexes. These results highlight that a change in redox potential is necessary to induce the reductive dissolution of Fe-bound P in such a system, as pH adjustment alone is not enough to liberate P. However, any redox-driven mobilization approach needs to be thoroughly assessed for any possible environmental effects, particularly with respect to Fe^{2+} and P leaching and the associated risk of eutrophication. Overall, findings from this study on the redox-sensitive behavior of Fe–P interactions have significant ramifications for the long-term sustainable management of P in agroecosystems where Fe dominates.

4 Conclusion

This study highlights the application of biochar for effectively separating P into solid fractions, an effective means to reduce the pollution load and improve nutrient management. Coagulant ($FeCl_3$) and biochar, particularly iron-modified biochar, are effective media for stabilizing nutrients and lowering the leaching risk of nutrients. Nutrient stability was assessed using conductometric-, pH metric-, and M-III analyses. Solution pH, ZP, and IS were taken into consideration for these analyses. P^- complex stability and ligand exchange efficiency are strongly influenced by the degree of dissociation. This study further discusses the release behavior of macronutrients under the influence of different extractants. Among the extractants tested, CBD was found to be the most suitable for extracting P from cation-bridged P-phosphate and iron-bound P^-. The extractants were used to evaluate the long-term environmental nutrient loading potential or immediate fertility contributions. The environmental fate and ecological impacts of the released P^- are beyond the scope of this study. Future research with these solid materials in the soil matrix is needed to evaluate the potential applicability of this process under natural environments. This approach offers a promising strategy for P recovery from manure solids of different origins.

Author contributions

Krishna Yadav: writing – original draft, methodology, investigation, data curation, conceptualization. Chumki Banik: writing – review & editing, investigation, Santanu Bakshi: writing – review & editing, methodology, investigation, funding acquisition, conceptualization.

Conflicts of interest

The authors declare that they have no known competing financial interests or personal relationship that could have appeared to influence the work reported in this paper.

Data availability

The data supporting this article have been included as part of the supporting information (SI). Supplementary information is available. See DOI: **https://doi.org/10.1039/d5va00281h**.

Acknowledgements

This work was supported by the Agricultural and Food Research Initiative Competitive grant no. 2022-68014-36665 from the USDA National Institute of Food and Agriculture. We thank Prof. Patrick Johnson of the Department of Materials Science and Engineering for assistance with Raman Spectroscopy analysis, and Dr Warren Straszheim of the Materials Analysis and Research Laboratory, Iowa State University, for assistance with SEM-EDS and XRD analyses.

References

1 J. L. Yost, A. M. Schmidt, R. Koelsch and L. R. Schott, Effect of Swine Manure on Soil Health Properties: A Systematic Review, *Soil Sci. Soc. Am. J.*, 2022, **86**(2), 450–486, DOI: **10.1002/saj2.20359**.

2 J. Ferreira, L. Santos, M. Ferreira, A. Ferreira and I. Domingos, Environmental Assessment of Pig Manure Treatment Systems through Life Cycle Assessment: A Mini-Review, *Sustainability*, 2024, **16**(9), 1–18, DOI: **10.3390/su16093521**.

3 K. Yadav, S. Bakshi, C. Banik, D. S. Andersen and R. C. Brown, Assessing Biochar and Zeolite for Enhanced Agricultural Sustainability of Swine Manure, *J. Environ. Chem. Eng.*, 2024, **12**, 112987, DOI: **10.1016/j.jece.2024.112987**.

4 M. Hjorth, K. V. Christensen, M. L. Christensen and S. G. Sommer, Solid-Liquid Separation of Animal Slurry in Theory and Practice. A Review, *Agron. Sustain. Dev.*, 2010, **30**(1), 153–180, DOI: **10.1051/agro/2009010**.

5 K. Yadav, C. Banik and S. B. Bakshi, Zeolite, and Ferric Chloride Effectively Separate Phosphorus and Nitrogen (plus Potassium) in Swine Manure: A Coagulation-Flocculation-Sedimentation Approach, *Chemosphere*, 2025, **374**, 144214, DOI: **10.1016/j.chemosphere.2025.144214**.

6 B. O. Nardis, J. Santana Da Silva Carneiro, I. M. G. De Souza, R. G. De Barros and L. C. Azevedo Melo, Phosphorus Recovery Using Magnesium-Enriched Biochar and Its Potential Use as Fertilizer, *Arch. Agron. Soil Sci.*, 2021, **67**(8), 1017–1033, DOI: **10.1080/03650340.2020.1771699**.

7 C. Sun, H. Cao, C. Huang, P. Wang, J. Yin, H. Liu, H. Tian, H. Xu, J. Zhu and Z. Liu, Eggshell Based Biochar for Highly Efficient Adsorption and Recovery of Phosphorus from Aqueous Solution: Kinetics, Mechanism and Potential as Phosphorus Fertilizer, *Bioresour. Technol.*, 2022, **362**, 127851, DOI: **10.1016/j.biortech.2022.127851**.

8 S. Ji, F. Zhang, P. Yao, C. Li, M. Faheem, Q. Feng, M. Chen and B. Wang, Optimization of Pig Manure-Derived Biochar for Ammonium and Phosphate Simultaneous Recovery from Livestock Wastewater, *Environ. Sci. Pollut. Res.*, 2023, **30**(34), 82532–82546, DOI: **10.1007/s11356-023-28092-w**.

9 T. Zhang, Q. Wang, Y. Deng and R. Jiang, Recovery of Phosphorus from Swine Manure by Ultrasound/H2O2 Digestion, Struvite Crystallization, and Ferric Oxide Hydrate/Biochar Adsorption, *Front. Chem.*, 2018, **6**, 1–15, DOI: **10.3389/fchem.2018.00464**.

10 D. G. Strawn, A. R. Crump, D. Peak, M. Garcia-Perez and G. Möller, Reactivity of Fe-Amended Biochar for Phosphorus Removal and Recycling from Wastewater, *PLOS Water*, 2023, **2**(4), e0000092, DOI: **10.1371/journal.pwat.0000092**.

11 K. Malhotra, J. Lamba, T. R. Way, C. Williams, K. G. Karthikeyan, R. Prasad, P. Srivastava and J. Zheng, Investigating the Effect of Animal Manure on Colloidal-Facilitated Phosphorus Transport, *Geoderma*, 2025, **455**, 117203, DOI: **10.1016/j.geoderma.2025.117203**.

12 S. Khan, C. Liu, P. J. Milham, K. M. Eltohamy, Y. Hamid, J. Jin, M. He and X. Liang, Nano and Micro Manure Amendments Decrease Degree of Phosphorus Saturation and Colloidal Phosphorus Release from Agriculture Soils, *Sci. Total Environ.*, 2022, **845**, 157278, DOI: 10.1016/j.scitotenv.2022.157278.

13 R. Sharma, R. W. Bella and M. T. F. Wong, Dissolved Reactive Phosphorus Played a Limited Role in Phosphorus Transport via Runoff, Throughflow and Leaching on Contrasting Cropping Soils from Southwest Australia, *Sci. Total Environ.*, 2017, **577**, 33–44, DOI: 10.1016/j.scitotenv.2016.09.182.

14 F. J. Stevenson, *Humus Chemistry: Genesis, Composition, Reactions*, John Wiley & Sons, New York, USA, 2nd edn, 1994.

15 M. von Lützow, I. Kögel-Knabner, K. Ekschmitt, H. Flessa, G. Guggenberger, E. Matzner and B. Marschner, SOM Fractionation Methods: Relevance to Functional Pools and to Stabilization Mechanisms, *Soil Biol. Biochem.*, 2007, **39**(9), 2183–2207, DOI: 10.1016/j.soilbio.2007.03.007.

16 H. Van Dijk, Cation Binding of Humic Acids, *Geoderma*, 1971, **5**(1), 53–67, DOI: 10.1016/0016-7061(71)90024-3.

17 Y. J. Shih, R. R. M. Abarca, M. D. G. de Luna, Y. H. Huang and M. C. Lu, Recovery of Phosphorus from Synthetic Wastewaters by Struvite Crystallization in a Fluidized-Bed Reactor: Effects of PH, Phosphate Concentration and Coexisting Ions, *Chemosphere*, 2017, **173**, 466–473, DOI: 10.1016/j.chemosphere.2017.01.088.

18 L. Zang, G. Tian, X. Liang, J. Liu and G. Peng, Effect of Water-Dispersible Colloids in Manure on the Transport of Dissolved and Colloidal Phosphorus through Soil Column, *African J. Agric. Res.*, 2011, **6**(30), 6369–6376, DOI: 10.5897/AJAR11.1520.

19 R. Kumar, J. Lamba, S. Adhikari, N. Kasera and H. A. Torbert, Influence of Iron-Modified Biochar on Phosphate Transport and Deposition in Saturated Porous Media under Varying PH, Ionic Strength, and Biochar Dosage, *Chemosphere*, 2025, **370**, 143932, DOI: 10.1016/j.chemosphere.2024.143932.

20 M. L. Christensen and S. G. Sommer, *Manure Characterisation and Inorganic Chemistry*, 2013, 41–65, DOI: 10.1002/9781118676677.ch4.

21 Q. Yang, X. Wang, W. Luo, J. Sun, Q. Xu, F. Chen, J. Zhao, S. Wang, F. Yao, D. Wang, X. Li and G. Zeng, Effectiveness and Mechanisms of Phosphate Adsorption on Iron-Modified Biochars Derived from Waste Activated Sludge, *Bioresour. Technol.*, 2018, **247**, 537–544, DOI: 10.1016/j.biortech.2017.09.136.

22 Y. Manawi, R. Al-Gaashani, S. Simson, Y. Tong, J. Lawler and V. Kochkodan, Adsorptive Removal of Phosphate from Water with Biochar from Acacia Tree Modified with Iron and Magnesium Oxides, *Sci. Rep.*, 2024, **14**(1), 1–20, DOI: 10.1038/s41598-024-66965-3.

23 S. Bakshi, D. A. Laird, R. G. Smith and R. C. Brown, Capture and Release of Orthophosphate by Fe-Modified Biochars: Mechanisms and Environmental Applications, *ACS Sustain. Chem. Eng.*, 2021, **9**(2), 658–668, DOI: 10.1021/acssuschemeng.0c06108.

24 C. Banik, S. Bakshi, D. S. Andersen, D. A. Laird, R. G. Smith and R. C. Brown, The Role of Biochar and Zeolite in Enhancing Nitrogen and Phosphorus Recovery: A Sustainable Manure Management Technology, *Chem. Eng. J.*, 2023, **456**, 141003, DOI: 10.1016/j.cej.2022.141003.

25 D. Fangueiro, C. Lopes, S. Surgy and E. Vasconcelos, Effect of the Pig Slurry Separation Techniques on the Characteristics and Potential Availability of N to Plants in the Resulting Liquid and Solid Fractions, *Biosyst. Eng.*, 2012, **113**(2), 187–194, DOI: 10.1016/j.biosystemseng.2012.07.006.

26 H. Wang, J. Dai, H. Chen, F. Wang, Y. Zhu, J. Liu, B. Zhou and R. Yuan, Adsorption of Phosphate by Mg/Fe-Doped Wheat Straw Biochars Optimized Using Response Surface Methodology: Mechanisms and Application in Domestic Sewage, *Environ. Eng. Res.*, 2023, **28**(2), 0–2, DOI: 10.4491/eer.2021.602.

27 T. A. O. K. Meetiyagoda, T. Takahashi and T. Fujino, Response Surface Optimization of Chemical Coagulation for Solid–Liquid Separation of Dairy Manure Slurry through Box–Behnken Design with Desirability Function, *Heliyon*, 2023, **9**(7), e17632, DOI: 10.1016/j.heliyon.2023.e17632.

28 K. Z. Abdiyev, Z. Toktarbay, A. Z. Zhenissova, M. B. Zhursumbaeva, R. N. Kainazarova and N. Nuraje, Colloids and Surfaces A : Physicochemical and Engineering Aspects The New Effective Flocculants – Copolymers of N , N-Dimethyl-N , N-Diallyl-Ammonium Chloride And, *Colloids Surf., A*, 2015, **480**, 228–235, DOI: 10.1016/j.colsurfa.2015.04.025.

29 J. Li, X. Song, J. Pan, L. Zhong, S. Jiao and Q. Ma, Adsorption and Flocculation of Bentonite by Chitosan with Varying Degree of Deacetylation and Molecular Weight, *Int. J. Biol. Macromol.*, 2013, **62**, 4–12, DOI: 10.1016/j.ijbiomac.2013.08.009.

30 A. C. Ferrari and J. Robertson, Interpretation of Raman Spectra of Disordered and Amorphous Carbon A, *Phys. Rev. B: Condens. Matter Mater. Phys.*, 2000, **31**(2), 632–645, DOI: 10.1007/BF02543692.

31 A. Sadezky, H. Muckenhuber, H. Grothe, R. Niessner and U. Pöschl, Raman Microspectroscopy of Soot and Related Carbonaceous Materials: Spectral Analysis and Structural Information, *Carbon*, 2005, **43**(8), 1731–1742, DOI: 10.1016/j.carbon.2005.02.018.

32 Y. Gao, M. Yan and G. V. Korshin, Effects of Ionic Strength on the Chromophores of Dissolved Organic Matter, *Environ. Sci. Technol.*, 2015, **49**(10), 5905–5912, DOI: 10.1021/acs.est.5b00601.

33 Y. Audette, D. S. Smith, C. T. Parsons, W. Chen, F. Rezanezhad and P. Van Cappellen, Phosphorus Binding to Soil Organic Matter via Ternary Complexes with Calcium, *Chemosphere*, 2020, **260**, 127624, DOI: 10.1016/j.chemosphere.2020.127624.

34 M. L. Christensen, M. Hjorth and K. Keiding, Characterization of Pig Slurry with Reference to Flocculation and Separation, *Water Res.*, 2009, **43**(3), 773–783, DOI: 10.1016/j.watres.2008.11.010.

35 A. M. Smith, U. Ekpo and A. B. Ross, The Influence of PH on the Combustion Properties of Bio-Coal Following Hydrothermal Treatment of Swine Manure, *Energies*, 2020, **13**(2), 1–20, DOI: **10.3390/en13020331**.
36 W. L. Lindsay, *Chemical Equilibria in Soils*, John Wiley and Sons Ltd, 1981.
37 S. R. Olesen, *Estimation of Available Phosphorus in Soils by Extraction with Sodium Bicarbonate; USDA Circular No. 939*, U.S. Goverment printing Office, Washington, D.C., 1954.
38 A. N. Sharpley, R. W. McDowell and P. J. A. Kleinman, Amounts, Forms, and Solubility of Phosphorus in Soils Receiving Manure, *Soil Sci. Soc. Am. J.*, 2005, **69**(4), 1355, DOI: **10.2136/sssaj2005.0078le**.
39 T. Borch, R. Kretzschmar, A. Skappler, P. Van Cappellen, M. Ginder-Vogel, A. Voegelin and K. Campbell, Biogeochemical Redox Processes and Their Impact on Contaminant Dynamics, *Environ. Sci. Technol.*, 2010, **44**(1), 15–23, DOI: **10.1021/es9026248**.
40 Y. Peng, T. Zhang, B. Tang, X. Li, S. Cui, C. Y. Guan, B. Zhang and Q. Chen, Interception of Fertile Soil Phosphorus Leaching with Immobilization Materials: Recent Progresses, Opportunities and Challenges, *Chemosphere*, 2022, **308**, 136337, DOI: **10.1016/j.chemosphere.2022.136337**.
41 *Extracting Phosphorus from Soil Using the Olsen Bicarbonate Method*, 2017, pp. , pp. 4–7. **https://gradcylinder.org/post/extracting-phosphorus-olsen-bicarbonate/#chemistry**.
42 O. A. Diaz, K. R. Reddy and P. A. Moore, Solubility of Inorganic Phosphorus in Stream Water as Influenced by PH and Calcium Concentration, *Water Res.*, 1994, **28**(8), 1755–1763, DOI: **10.1016/0043-1354(94)90248-8**.
43 D. L. Sparks, *Environmental Soil Chemistry: An Overview*, 1995, pp. 1–42, DOI: **10.1016/b978-0-12-656445-7.50005-x**.
44 O. P. Mehra and M. L. Jackson, Iron Oxide Removal From Soils and Clays By a Dithionite–Citrate System Buffered With Sodium Bicarbonate, *Clays Clay Miner.*, 1958, 317–327, DOI: **10.1016/b978-0-08-009235-5.50026-7**.